



# CHORUS

This is the accepted manuscript made available via CHORUS. The article has been published as:

## Signatures of Andreev Blockade in a Double Quantum Dot Coupled to a Superconductor

Po Zhang, Hao Wu, Jun Chen, Sabbir A. Khan, Peter Krogstrup, David Pekker, and Sergey  
M. Frolov

Phys. Rev. Lett. **128**, 046801 — Published 25 January 2022

DOI: [10.1103/PhysRevLett.128.046801](https://doi.org/10.1103/PhysRevLett.128.046801)

# Signatures of Andreev blockade in a double quantum dot coupled to a superconductor

Po Zhang,<sup>1</sup> Hao Wu,<sup>1</sup> Jun Chen,<sup>2</sup> Sabbir A. Khan,<sup>3,4</sup> Peter Krogstrup,<sup>3,4</sup> David Pekker,<sup>1</sup> and Sergey M. Frolov<sup>1,\*</sup>

<sup>1</sup>*Department of Physics and Astronomy, University of Pittsburgh, Pittsburgh, PA, 15260, USA*

<sup>2</sup>*Department of Electrical and Computer Engineering, University of Pittsburgh, Pittsburgh, PA, 15260, USA*

<sup>3</sup>*Microsoft Quantum Materials Lab Copenhagen, 2800 Lyngby, Denmark*

<sup>4</sup>*Center for Quantum Devices, Niels Bohr Institute, University of Copenhagen, 2100 Copenhagen, Denmark*

We investigate an electron transport blockade regime in which a spin-triplet localized in the path of current is forbidden from entering a spin-singlet superconductor. To stabilize the triplet a double quantum dot is created electrostatically near a superconducting Al lead in an InAs nanowire. The quantum dot closest to the normal lead exhibits Coulomb diamonds, the dot closest to the superconducting lead exhibits Andreev bound states and an induced gap. The experimental observations compare favorably to a theoretical model of Andreev blockade, named so because the triplet double dot configuration suppresses Andreev reflections. Observed leakage currents can be accounted for by finite temperature. We observe the predicted quadruple level degeneracy points of high current and a periodic conductance pattern controlled by the occupation of the normal dot. Even-odd transport asymmetry is lifted with increased temperature and magnetic field. This blockade phenomenon can be used to study spin structure of superconductors. It may also find utility in quantum computing devices that utilize Andreev or Majorana states.

Andreev bound states (ABSs) in semiconductor quantum dots (QDs) coupled to superconducting contacts are a subject of active investigation [1–4]. A transition between singlet and doublet spin (or even-odd parity) ground states has been mapped experimentally and understood theoretically in single Andreev quantum dots [1, 2, 5]. ABS are related to Majorana zero modes and topological qubits [6–12]. While these qubits have not been achieved, other types of qubits namely Andreev, fluxonium and transmon have all been created in superconductor-semiconductor nanostructures [13–17]. Spin qubits can also be hosted in semiconductor nanowires without superconducting contacts [18–20]. QDs exhibit iconic blockade phenomena: Coulomb blockade used in metrology [21], Pauli spin blockade [22] used for spin qubit operation [23].

Here we ask a question: can a blockade phenomenon unique to superconductors, Andreev blockade (AB) [24], be demonstrated? The basic principle is that electrons can only enter the superconducting lead as spin-singlet Cooper pairs (Fig. 1(a)). In the DQD at zero field, the four (1,1) states (three triplets, a singlet) are nearly degenerate. Any one of the four can be occupied stochastically. While a singlet will form a Cooper pair and enter the superconductor, any of the three triplets will be impeded on the dot, and as soon as a triplet is filled the blockade is established, typically at a sub-nanosecond timescale [18, 22, 23, 25]. Soft induced gap, magnetic impurities, triplet superconductivity, or a combination of effective spin-orbit coupling (SOC) and magnetic field are expected to lift this blockade [26, 27].

We fabricate a DQD in an InAs nanowire with an Al shell (Fig. 1(b)). The right side of the DQD is connected to a superconductor (QD<sub>S</sub>), the left to a non-superconductor lead, such that QD<sub>N</sub> is a nor-

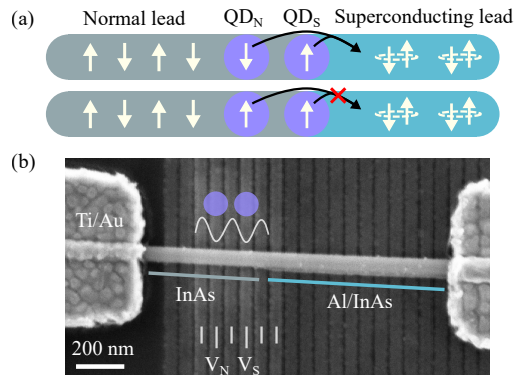


FIG. 1. (a) Schematic of AB. The blocked configuration is indicated with a red cross showing how a spin-triplet in DQD is prevented from forming a spin-singlet Cooper pair. (b) SEM image of a device similar to the one studied in the main text. Section marked ‘Al/InAs’ is an InAs nanowire covered by an Al shell. A section where the shell is etched is marked ‘InAs’. Vertical lines mark gate electrodes used in creating the DQD, other visible gates are floating.

mal dot. QD<sub>S</sub> exhibits an induced gap and ABSs (Figs. 2(a,b)). QD<sub>N</sub> is characterized by Coulomb diamonds (Figs. 2(c,d)). Subgap transport reveals patterns that theory predicted for the four-step Andreev charge-transport cycle which arises when two electrons required to form a Cooper pair are transported through the DQD (Fig. 3). As a signature of AB we find asymmetry between quadruple degeneracy points (DPs) at even-to-odd and odd-to-even transitions in the normal dot (Figs. 3,4). The observed asymmetry has the properties predicted by theory [24]: the pattern is flipped at opposite voltage bias and it disappears at higher temperature or magnetic field (Figs. 5,S4). Experimentally, we find that current is not

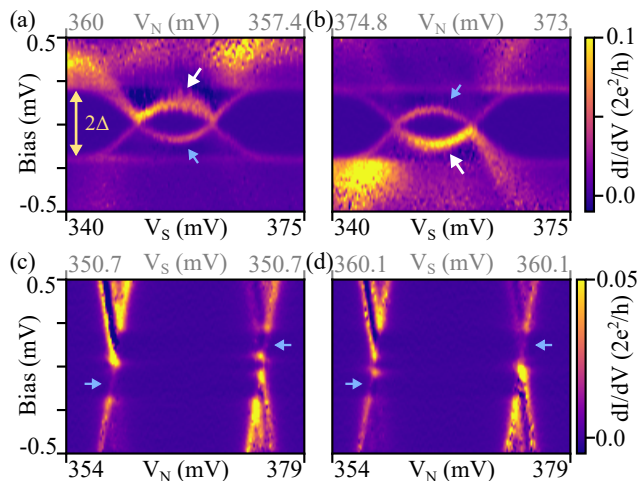


FIG. 2. Differential conductance spectra for (a-b)  $QD_S$  and (c-d)  $QD_N$ . Spectra are taken by fixing one dot at a degenerate state while tuning the other dot with the  $(V_S, V_N)$  combination. Voltage combinations are indicated in Fig. 3(a). Large arrows and small arrows indicate resonance peaks with different amplitudes.

completely blocked in the regimes that we label as AB. Our numerical model accounts for this by introducing finite temperature.

Fig. 1(b) shows a typical device. An InAs nanowire covered with 15 nm epitaxial Al is placed on top of 60 nm pitch gates. The DQD is defined by voltages on gates indicated in the image.  $V_N$  and  $V_S$  are voltages primarily used for tuning dots. Al on the left section of the wire is selectively etched to make the normal lead. The device is measured in a dilution fridge with a base temperature of about 40 mK. The typical material parameters are as follows. The superconducting gap of Al is about 0.2 meV, the SOC length in bare InAs nanowires is 100-300 nm, the  $g$ -factor in InAs is of order 10. A triplet component may be present in superconductors with strong SOC [27]. However, no direct evidence has been reported in the Al/InAs system yet.

We demonstrate that while  $QD_S$  exhibits ABSs, dot  $QD_N$  exhibits Coulomb diamonds, which are a staple of non-superconducting QD transport (Fig. 2). The DQD configuration is set up by tuning gates adjacent to the superconducting lead. Spectra are taken by fixing one dot at a DP while tuning the other.  $QD_S$  shows induced hard gap which is a stripe of suppressed current below  $\Delta/e = 0.2$  mV, consistent with earlier works [28–31]. Inside the gap, loop-like resonances are observed. Such resonances have been reported experimentally and theoretically as originating from ABS [1]. We produce a spectrum similar to Ref. [1] in the supplementary information (SI) indicating that our model is in agreement with the established theory on the ABS spectra in QDs coupled to superconductors.  $QD_N$  show Coulomb diamonds and no clear induced gap. Fig. 3(a) shows traces

corresponding to these spectra.

There are also more subtle conditions the system must meet for observing AB. The induced gap should be hard to suppress subgap single-particle transport, which is an AB lifting mechanism. The barrier to the superconducting lead should be low to induce ABSs. This is in contrast with Pauli blockade which typically require few electron regimes and hence high barriers to facilitate strong confinement. The inter-dot charging energy should be smaller than the induced gap because the Andreev transport regions shrink rapidly with the increasing inter-dot charging energy [24]. To match experimental results we set the inter-dot charging energy to 10  $\mu$ eV, which corresponds to a weakly coupled regime.

Predicted Signatures of AB. Following Ref. [24], we are looking for following signatures of AB. We describe charge states by parities. The parity in  $QD_N$  can be inferred by shifting of DPs in magnetic field, with odd (even) region expanding (shrinking) at higher fields (Fig. S9). The parity in  $QD_S$  can be inferred from Andreev spectra, with regions inside loop-like resonances odd (Fig. 2(a)-(b)). See SI and Ref. [24] for theoretical background.

- (A) At subgap biases current is confined to triangular regions of the charge stability diagram. The triangles do not appear in closely spaced pairs as in non-superconducting DQDs where they form around triple DPs. Instead, triangles appear at quadruple Andreev DPs, a consequence of the two-electron transfer cycle.
- (B) An alternating pattern of blockade/no-blockade is observed when quadruple points are tuned by  $V_N$ .  $V_S$  does not affect whether blockade is present or not.
- (C) The sign of source-drain bias voltage flips AB. A DP that is blockaded in positive bias is not blockaded in negative bias, and vice versa.
- (D) AB is not present when superconductivity is suppressed by magnetic field or temperature. Signatures (A)-(C) should no longer be manifest.

Signatures (B) and (C) can be formulated together as follows. AB is expected for (odd,odd) $\rightarrow$ (even,even) and (odd,even) $\rightarrow$ (even,odd) transitions, where  $(P_N, P_S)$  stand for parities in  $QD_N$  and  $QD_S$ , the arrows indicate the direction of charge transfer, so that the conditions are valid for both signs of bias. In SI, we provide diagrams illustrating charge transfer cycles at four DPs, both those that result in AB as well as those that do not.

An ideal blockade corresponds to total suppression of current below the gap. Blockade can be suppressed by the presence of sub-gap and thermally-excited quasiparticles [24]. If AB is only partially suppressed, a reduced current (leakage current) indicates blockade.

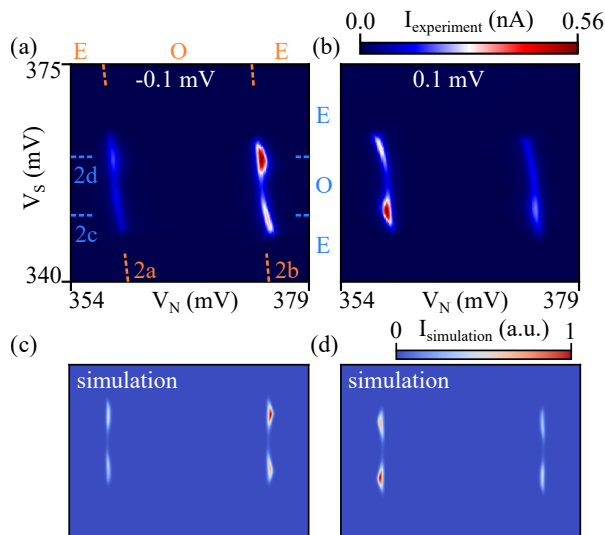


FIG. 3. (a-b) Experimental and (c-d) simulated results of a "unit" stability diagram with  $2 \times 2$  quadruple DPs. Parities in  $QD_N$  and  $QD_S$  are labeled on top and right axes in panel (a) (E - even, O - odd). Dashed lines indicate traces along which spectra in Fig. 2 are taken. The bias is indicated in white. Parameters for simulation (in a.u. which match system energies in meV for convenience): source-drain bias  $\mu_S - \mu_N = -0.1$  in (c), 0.1 in (d), charging energy  $U_N = 4$ ,  $U_S = 0.7$ , inter-dot charging energy  $U_{NS} = 0.01$ , induced gap  $\Delta_S = 0.2$ , temperature  $T = 0.02$ .

In principle there should be no fine-tuning required to observe AB. All needed is one normal dot, one superconducting dot and a hard gap superconductor lead. Thus we are looking for a  $V_S - V_N$  region including many DPs that exhibit blockade signatures. In practice, mesoscopic factors such as additional QDs in segments covered by leads can also introduce current modulations. Thus some gate tuning may still be required to clearly observe AB.

**Measured AB Signatures.** Signature (A) which is current confined to single, not double, triangles in the stability diagram is illustrated by Figs. 3(a,b). Stability diagrams are taken at two opposite voltages. For both bias directions we observe elongated triangles, rounded due to relatively low voltages required to stay below the induced gap. Numerical results in Figs. 3(c,d) closely reproduce the experiment. Larger gate range (Fig. 4) confirms the single-triangle character of the DPs, *though it displays a greater variety of triangle shapes than Fig. 3.*

Signature (B) in experiment presents itself as an alternating pattern of high current/low current when the occupation of  $QD_N$  is changed. It is illustrated by Figs. 3 and 4. We see dim DPs followed by bright ones. In Fig. 4 the dim (bright) columns are marked by dim (bright) arrows. The region depicted contains  $6 \times 6$  DPs. *This is the largest continuous regime we found for AB.*

All DPs are detectable, even those supposed to be blocked. In the context of AB this means the block-

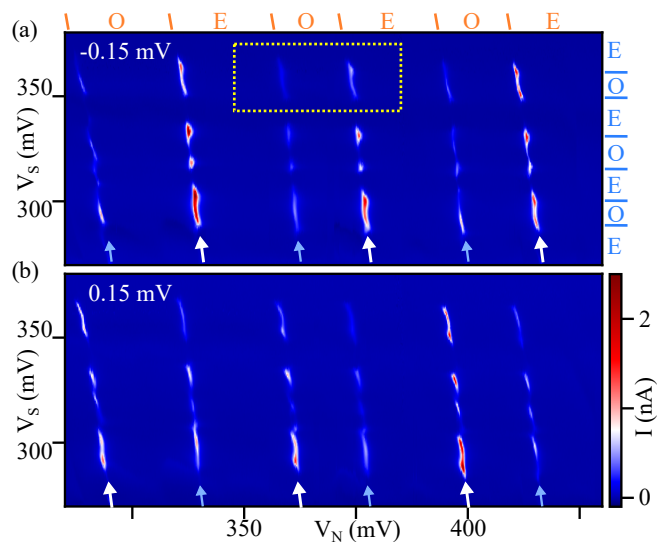


FIG. 4. Stability diagrams in a larger ( $V_S, V_N$ ) parameter space. The dashed rectangle in panel (a) encloses the region studied in Figs. 2, 3 and 5. Parities in  $QD_N$  ( $QD_S$ ) is labeled on top (right) axis. Blue (white) arrows indicate columns of conductance triangles with low (high) current. Bias is indicated in white.

ade is partially lifted. In the simulation (Figs. 3(c,d)) we assume finite temperature to reproduce this behavior. Finite temperature enables single particle tunneling into the hard-gap via thermally excited quasi-particles, and provides a way around the blocked Andreev processes. *While softened gap does account for the observation on a qualitative level, spin non-conserving processes can also lift AB. We point out that no significant magnetic impurities were found in epitaxial Al/InAs nanowires [28, 31]. SOC does not lift triplet blockade at zero magnetic field [25], but can do so at finite field. Spin relaxation mediated by phonons or hyperfine interaction can be other possible factors [32]. To study these effects we would use a superconductor with a larger gap to rule out gap softening and expand temperature/field range of AB.*

Signature (C) is the reversal of the high/low current pattern in opposite bias (Fig. 3). At  $-0.1$  ( $+0.1$ ) mV, current is smaller for DPs on the left (right). Simulation shows good agreement with this observation (Figs. 3(c,d)). The same behavior largely holds in Figs. 4 over an expanded range.

Bias asymmetry can also be seen in Fig. 2. In the upper panels, Andreev loops have non-symmetric amplitudes between positive and negative voltages: either the upper or the lower half of the loop is brighter. In Coulomb diamonds (lower panels), the pattern of intensity is anti-symmetric with respect to the center of the figure. For example, in panel 2(c), the left (right) region is bright at positive (negative) bias - when looking at biases below the gap. These patterns are consistent



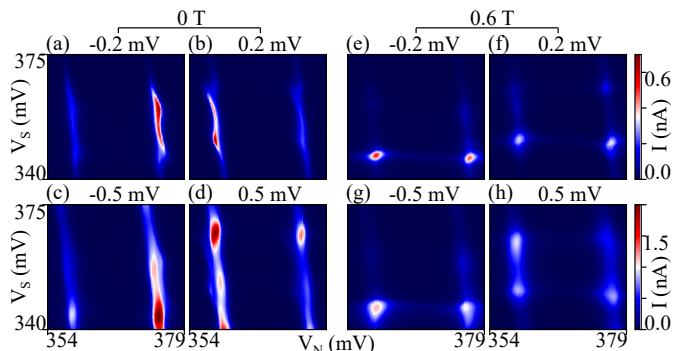


FIG. 5. Stability diagrams at different biases and fields (a-d)  $B = 0$  and (e-h)  $0.6$  T. The bias is indicated in black. The magnetic field is in the sample plane at a 24 degree angle with the nanowire.

with AB: the occupation of  $QD_S$  does not affect AB, the occupation of  $QD_N$  flips AB to the opposite bias.

Finally, signature (D) which is the disappearance of other signatures when superconductivity is suppressed is presented in Fig. 5 and Figs. S4, S8, S11, S12. Figs. 5(a-d) reproduce the same regime as in Fig. 3 for different biases. At  $0.6$  T, we observe that the alternating patterns of bright/dim DPs are no longer present, neither is the bias asymmetry. Magnetic field introduces subgap density of states at fields below the critical field, leading to the lifting of AB. For thin Al shell, it is reasonable to expect this at fields of several hundred millitesla for a field at an approximately 30 degree angle with the nanowire [33]. The bright/dim pattern also vanishes at elevated temperature (Fig. S4).

Elongated DPs are replaced by less elongated points at higher fields where superconductivity of the aluminum shell is suppressed (Figs. 5(e-h)). In this regime the DPs appear more similar to those of a normal DQD. Though two triangles corresponding to two triple points cannot be resolved due to rounding and relatively weak interdot capacitive coupling [34]. In future experiments using a larger gap superconductor such as Sn or Pb [31, 35, 36] can provide a larger bias range for AB and make this observation more clear by reducing the relative role of feature broadening. These materials also have stronger SOC than Al in which case AB can be used to explore the effect of metallic spin-orbit on spin-resolved transport across superconductor-semiconductor interfaces.

Alternative explanations. In this section we provide alternative interpretations that we cannot fully exclude. We also give our reasoning for favoring AB over these explanations. The full AB signatures from the previous section is our main argument. Here we are providing narrower considerations focused on alternative scenarios.

Part of the signatures we present in favor of AB is the asymmetric conductance in the direction of bias. Asymmetric conductance is commonplace in hybrid structures and QDs without superconducting contacts [1, 2, 5, 34,

37]. The most common kind of asymmetry is when resonances of one slope are brighter in Coulomb diamond data (see, e.g., Fig. S6), typically due to unequal barrier strengths. In Andreev QDs this manifests resonances enhancing parts of the Andreev loops, for instance the top right and the bottom left. AB enhances conductance asymmetrically along the zero-bias line: e.g. top part of the loop is bright, bottom part is dim.

Bias asymmetries are observed in our data at voltages above the gap. However, Figs. S5, S6 illustrate that in general asymmetry at high bias does not follow the same pattern as subgap low-bias asymmetry, suggesting they have different origin.

We have considered the possibility that signatures (A-D) were only identified due to fine-tuning in a deliberate search for predicted patterns. In this scenario, signatures such as alternating bright/dim DPs and bias asymmetries are not due to AB, but rather they arise accidentally due to additional states co-existing in the nanowire - for example spurious QDs in lead segments. Those other states are fine-tuned to modulate transport in the DQD in just the right way to be consistent with AB.

We cannot fully exclude the possibility of the presence of extra states beyond the two QDs. We see, e.g. Fig. 4 lower left part, that while the stability points form a dominating double-dot pattern, their intensities vary across a large  $V_S$ - $V_N$  range suggesting non-monotonic coupling to states outside the dots or non-monotonic inter-dot barriers. This is typical for QDs, including those made in the Intel cleanroom [38].

Additional data (SI) and full data [39] also demonstrate that within the same device other regimes do not show patterns of AB, when gates are set differently.

Our argument to not favor the above explanation is that a pattern consistent with AB signatures (A-C) are observed over a regime covering  $6 \times 6$  DPs, in several sufficiently different DQD configurations, and, in a more limited range in other devices. Furthermore, the fact that bias asymmetry and alternating current patterns disappear when superconductivity is suppressed (signature D) convinces us that these phenomena have to do with subgap superconducting transport which is the regime of Andreev reflection.

Recently larger hard-gaps have been induced in nanowires with tin and lead [35, 36]. It would be interesting to repeat AB experiments using these superconductors. First, larger gap-to-measurement-temperature ratio may result in stronger blockade. Second, the ability to work at higher bias and larger charging energies would make the observation of blockade features such as bias triangles more conclusive, and reduce the role of rounding at low biases. Finally, blockade can be studied to higher fields allowing for a detailed investigation of spin pairing in the superconductor.

Several improvements can be done in follow-on work related to materials processing. This would impact not

only AB experiments but many works aimed at searching for Majorana modes and building superconductor-semiconductor qubits. For instance, the wet etch degrades the quality of nanowires by introducing defects [31, 40]. The use of in-situ shadowing are promising to explore.

AB offers a means of studying spin-resolved transport in hybrid devices at zero field. We foresee application of AB in experiments that probe spin pairing in superconductors. Much like Pauli blockade was used to investigate spin mixing mechanisms in semiconductors, AB can be potentially used to detect triplet pairing or admixtures thereof, spin-flip scattering, spin polarization or textures such as Larkin-Ovchinnikov-Fulde-Ferrel state in superconductors. A two-arm AB device with two DQDs in parallel can in principle be used as a spin-sensitive probe for crossed Andreev reflection. QDs with superconducting leads are building blocks of Andreev qubits, Kitaev emulators and topological qubits [12, 15, 41]. These devices may manifest AB or utilize it to detect the state of a qubit or an emulator by providing a spin-dependent transport or transition rate element.

Several versions of a triplet blockade in QDs closely related to AB have been considered theoretically [42–46], with several works focusing on a parallel combination of QDs, which is relevant for crossed Andreev reflection [47–49]. Other types of blockade related to Andreev reflection such as chiral blockade have been proposed [50].

A recent experiment in a similar DQD setup with two rather than one superconducting lead has studied a triplet blockade that develops at large fields, where spin triplet is the unique ground state of the DQD [51]. In contrast, AB demonstrated in this work occurs at zero field, due to the stochastic filling of a QD by random spins.

S.F. and D.P. are supported by NSF PIRE-1743717. S.F. is supported by NSF DMR-1906325, ONR and ARO. P.K. is supported by European Union Horizon 2020 research and innovation program under the Marie Skłodowska-Curie Grant No. 722176 (INDEED), Microsoft Quantum and the European Research Council (ERC) under Grant No. 716655 (HEMs-DAM).

## REFERENCES

- 
- \* frolovsm@pitt.edu
- [1] R. S. Deacon, Y. Tanaka, A. Oiwa, R. Sakano, K. Yoshida, K. Shibata, K. Hirakawa, and S. Tarucha, *Phys. Rev. Lett.* **104**, 076805 (2010).
  - [2] E. J. Lee, X. Jiang, M. Houzet, R. Aguado, C. M. Lieber, and S. De Franceschi, *Nature nanotechnology* **9**, 79 (2014).
  - [3] J. A. Sauls, *Philosophical Transactions of the Royal Society A: Mathematical, Physical and Engineering Sciences* **376**, 20180140 (2018).
  - [4] E. Prada, P. San-Jose, M. W. de Moor, A. Geresdi, E. J. Lee, J. Klinovaja, D. Loss, J. Nygård, R. Aguado, and L. P. Kouwenhoven, *Nature Reviews Physics* **2**, 575 (2020).
  - [5] Z. Su, R. Žitko, P. Zhang, H. Wu, D. Car, S. R. Plissard, S. Gazibegovic, G. Badawy, M. Hocevar, J. Chen, E. P. A. M. Bakkers, and S. M. Frolov, *Phys. Rev. B* **101**, 235315 (2020).
  - [6] A. Kitaev, *Annals of Physics* **303**, 2 (2003).
  - [7] C. Nayak, S. H. Simon, A. Stern, M. Freedman, and S. Das Sarma, *Rev. Mod. Phys.* **80**, 1083 (2008).
  - [8] V. Mourik, K. Zuo, S. M. Frolov, S. R. Plissard, E. P. A. M. Bakkers, and L. P. Kouwenhoven, *Science* **336**, 1003 (2012).
  - [9] M. T. Deng, S. Vaitiekenas, E. B. Hansen, J. Danon, M. Leijnse, K. Flensberg, J. Nygård, P. Krogstrup, and C. M. Marcus, *Science* **354**, 1557 (2016).
  - [10] J. Alicea, Y. Oreg, G. Refael, F. von Oppen, and M. P. A. Fisher, *Nature Physics* **7**, 412 (2011).
  - [11] B. van Heck, A. R. Akhmerov, F. Hassler, M. Burrello, and C. W. J. Beenakker, *New Journal of Physics* **14**, 035019 (2012).
  - [12] T. Karzig, C. Knapp, R. M. Lutchyn, P. Bonderson, M. B. Hastings, C. Nayak, J. Alicea, K. Flensberg, S. Plugge, Y. Oreg, C. M. Marcus, and M. H. Freedman, *Phys. Rev. B* **95**, 235305 (2017).
  - [13] G. de Lange, B. van Heck, A. Bruno, D. J. van Woerkom, A. Geresdi, S. R. Plissard, E. P. A. M. Bakkers, A. R. Akhmerov, and L. DiCarlo, *Phys. Rev. Lett.* **115**, 127002 (2015).
  - [14] T. W. Larsen, K. D. Petersson, F. Kueemeth, T. S. Jespersen, P. Krogstrup, J. Nygård, and C. M. Marcus, *Phys. Rev. Lett.* **115**, 127001 (2015).
  - [15] M. Hays, G. de Lange, K. Serniak, D. J. van Woerkom, D. Bouman, P. Krogstrup, J. Nygård, A. Geresdi, and M. H. Devoret, *Phys. Rev. Lett.* **121**, 047001 (2018).
  - [16] F. Luthi, T. Stavenga, O. W. Enzing, A. Bruno, C. Dickel, N. K. Langford, M. A. Rol, T. S. Jespersen, J. Nygård, P. Krogstrup, and L. DiCarlo, *Phys. Rev. Lett.* **120**, 100502 (2018).
  - [17] M. Pita-Vidal, A. Bargerbos, C.-K. Yang, D. J. van Woerkom, W. Pfaff, N. Haider, P. Krogstrup, L. P. Kouwenhoven, G. de Lange, and A. Kou, *Phys. Rev. Applied* **14**, 064038 (2020).
  - [18] S. Nadj-Perge, S. M. Frolov, E. P. A. M. Bakkers, and L. P. Kouwenhoven, *Nature* **468**, 1084 (2010).
  - [19] K. D. Petersson, L. W. McFaul, M. D. Schroer, M. Jung, J. M. Taylor, A. A. Houck, and J. R. Petta, *Nature* **490**, 380 (2012).
  - [20] J. W. G. van den Berg, S. Nadj-Perge, V. S. Pribiag, S. R. Plissard, E. P. A. M. Bakkers, S. M. Frolov, and L. P. Kouwenhoven, *Phys. Rev. Lett.* **110**, 066806 (2013).
  - [21] M. W. Keller, *Metrologia* **45**, 102 (2008).
  - [22] K. Ono, D. Austing, Y. Tokura, and S. Tarucha, *Science* **297**, 1313 (2002).
  - [23] J. R. Petta, A. C. Johnson, J. M. Taylor, E. A. Laird, A. Jacoby, M. D. Lukin, C. M. Marcus, M. P. Hanson, and A. C. Gossard, *Science* **309**, 2180 (2005).
  - [24] D. Pekker, P. Zhang, and S. M. Frolov, *SciPost Phys.* **11**, 81 (2021).
  - [25] J. Danon and Y. V. Nazarov, *Phys. Rev. B* **80**, 041301

- (2009).
- [26] I. Žutić and S. Das Sarma, Phys. Rev. B **60**, R16322 (1999).
- [27] L. P. Gor'kov and E. I. Rashba, Physical Review Letters **87**, 037004 (2001).
- [28] P. Krogstrup, N. L. B. Ziino, W. Chang, S. M. Albrecht, M. H. Madsen, E. Johnson, J. Nygård, C. Marcus, and T. S. Jespersen, Nature Materials **14**, 400 (2015).
- [29] W. Chang, S. M. Albrecht, T. S. Jespersen, F. Kuemmeth, P. Krogstrup, J. Nygård, and C. M. Marcus, Nature Nanotechnology **10**, 232 (2015).
- [30] S. Gazibegovic, D. Car, H. Zhang, S. C. Balk, J. A. Logan, M. W. A. de Moor, M. C. Cassidy, R. Schmits, D. Xu, G. Wang, P. Krogstrup, R. L. M. Op het Veld, K. Zuo, Y. Vos, J. Shen, D. Bouman, B. Shojaei, D. Pennachio, J. S. Lee, P. J. van Veldhoven, S. Koelling, M. A. Verheijen, L. P. Kouwenhoven, C. J. Palmstrøm, and E. P. A. M. Bakkers, Nature **548**, 434 (2017).
- [31] S. A. Khan, C. Lampadaris, A. Cui, L. Stampfer, Y. Liu, S. J. Pauka, M. E. Cachaza, E. M. Fiordaliso, J.-H. Kang, S. Korneychuk, T. Mutas, J. E. Sestoft, F. Krizek, R. Tanta, M. C. Cassidy, T. S. Jespersen, and P. Krogstrup, ACS Nano **14**, 14605 (2020).
- [32] R. Hanson, L. P. Kouwenhoven, J. R. Petta, S. Tarucha, and L. M. K. Vandersypen, Rev. Mod. Phys. **79**, 1217 (2007).
- [33] Z. Su, A. Zarassi, J.-F. Hsu, P. San-Jose, E. Prada, R. Aguado, E. J. H. Lee, S. Gazibegovic, R. L. M. Op het Veld, D. Car, S. R. Plissard, M. Hocevar, M. Pendharkar, J. S. Lee, J. A. Logan, C. J. Palmstrøm, E. P. A. M. Bakkers, and S. M. Frolov, Phys. Rev. Lett. **121**, 127705 (2018).
- [34] Z. Su, A. B. Tacla, M. Hocevar, D. Car, S. R. Plissard, E. P. A. M. Bakkers, A. J. Daley, D. Pekker, and S. M. Frolov, Nature Communications **8**, 585 (2017).
- [35] M. Pendharkar, B. Zhang, H. Wu, A. Zarassi, P. Zhang, C. P. Dempsey, J. S. Lee, S. D. Harrington, G. Badawy, S. Gazibegovic, R. L. M. Op het Veld, M. Rossi, J. Jung, A.-H. Chen, M. A. Verheijen, M. Hocevar, E. P. A. M. Bakkers, C. J. Palmstrøm, and S. M. Frolov, Science **372**, 508 (2021).
- [36] T. Kanne, M. Marnauza, D. Olsteins, D. J. Carrad, J. E. Sestoft, J. de Bruijckere, L. Zeng, E. Johnson, E. Olsson, K. Grove-Rasmussen, *et al.*, arXiv preprint arXiv:2002.11641 (2020).
- [37] A. Jellinggaard, K. Grove-Rasmussen, M. H. Madsen, and J. Nygård, Physical Review B **94**, 064520 (2016).
- [38] A. Zwerver *et al.*, arXiv preprint arXiv:2101.12650 (2021).
- [39] DOI: 10.5281/zenodo.4446186.
- [40] D. J. Carrad, M. Bjergfelt, T. Kanne, M. Aagesen, F. Krizek, E. M. Fiordaliso, E. Johnson, J. Nygård, and T. S. Jespersen, Advanced Materials **32**, 1908411 (2020).
- [41] J. D. Sau and S. D. Sarma, Nature Communications **3**, 964 (2012).
- [42] M.-S. Choi, C. Bruder, and D. Loss, Phys. Rev. B **62**, 13569 (2000).
- [43] P. Recher, E. V. Sukhorukov, and D. Loss, Physical Review B **63**, 165314 (2001).
- [44] C. Padurariu and Y. V. Nazarov, EPL (Europhysics Letters) **100**, 57006 (2012).
- [45] S. Droste, S. Andergassen, and J. Splettstoesser, Journal of Physics: Condensed Matter **24**, 415301 (2012).
- [46] Y. Tanaka, N. Kawakami, and A. Oguri, Phys. Rev. B **81**, 075404 (2010).
- [47] J. Eldridge, M. G. Pala, M. Governale, and J. König, Phys. Rev. B **82**, 184507 (2010).
- [48] M. Leijnse and K. Flensberg, Phys. Rev. Lett. **111**, 060501 (2013).
- [49] Z. Scherübl, A. Pályi, and S. Csonka, Beilstein J. Nanotechnol. **10**, 363 (2019).
- [50] N. Bovenzi, M. Breitkreiz, P. Baireuther, T. E. O'Brien, J. Tworzydło, i. d. I. Adagideli, and C. W. J. Beenakker, Phys. Rev. B **96**, 035437 (2017).
- [51] D. Bouman, R. J. J. van Gulik, G. Steffensen, D. Pataki, P. Boross, P. Krogstrup, J. Nygård, J. Paaske, A. Pályi, and A. Geresdi, Phys. Rev. B **102**, 220505 (2020).
- [52] A. Zarassi, Z. Su, J. Danon, J. Schwenderling, M. Hocevar, B. M. Nguyen, J. Yoo, S. A. Dayeh, and S. M. Frolov, Phys. Rev. B **95**, 155416 (2017).
- [53] B. Cord, J. Lutkenhaus, and K. K. Berggren, Journal of Vacuum Science & Technology B: Microelectronics and Nanometer Structures Processing, Measurement, and Phenomena **25**, 2013 (2007).